Chaotic Time Series Prediction Using Brain Emotional Learning Based Recurrent Fuzzy System (BELRFS)

Mahboobeh Parsapoor*
School of Information Science, Computer and Electrical Engineering (IDE), Halmstad University,Halmstad, Sweden.
E-mail: mahpar11@student.hh.se
*Corresponding author

Urban Bilstrup
School of Information Science, Computer and Electrical Engineering (IDE), Halmstad University,Halmstad, Sweden
E-mail: urban.bilstrup@hh.se

Abstract: In this paper an architecture based on the anatomical structure of the emotional network in the brain of mammalians is applied as a prediction model for chaotic time series studies. The architecture is called BELRFS, which stands for: Brain Emotional Learning-based Recurrent Fuzzy System. It adopts neuro-fuzzy adaptive networksto mimic the functionality of brain emotional learning. In particular, the model is investigated to predict space storms, since the phenomenon has been recognized as a threat to critical infrastructure in modern society. To evaluate the performance of BELRFS, three benchmark time series: Lorenz time series, sunspot number time series and Auroral Electrojet (AE) index. The obtained results of BELRFS are compared with Linear Neuro-Fuzzy (LNF) with the Locally Linear Model Tree algorithm (LoLiMoT). The results indicate that the suggested model outperforms most of data driven models in terms of prediction accuracy.

Keywords: Brain emotional learning; Chaotic time series; Neuro-fuzzy adaptive networks; Linear Neuro-Fuzzy (LNF) with the Locally Linear Model Tree algorithm, Space weather forecasting; Solar activity forecasting.

1 INTRODUCTION

An accurate prediction of space weather is crucial to mitigate the harmful effects on critical infrastructure such as: satellites, telecommunication and power grid systems [Thompson, 1993; Schatten et al., 1993; Izeman et al., 1998; Golipour et al., 2004; 2006a; 2006b]. This can be done by providing early warning of super storms on the Sun [Kappenman 2012]. Space weather forecasting is conducted by quantitative-predictive measures and providing early warnings of extreme space weather events. This paper will focus upon the prediction of solar activity and geomagnetic storms, by using the Brain Emotional Learning-based Recurrent Fuzzy System (BELRFS).

Data driven methods have long been used for the prediction and identification of chaotic systems, in particular, the biologically inspired methods, e.g. neural network models and neuro-fuzzy methods. These approaches have a high generalization capability, which make them popular for predicting chaotic time series. However, to achieve high accuracy in the predictions, these methods often require a very large set of training data. Thus, they are not desirable for chaotic time series prediction with a limited training data samples. Another significant issue of these methods is the computational complexity.

Brain emotional learning-based methodologies [Lucas et al., 2003; Lucas et al., 2004; Parsapoor et al., 2008; 2012a; 2012b] have been developed to address the above mentioned issues. They have simple structure with a lower computational complexity if compared with neural network

and neuro-fuzzy methods [Babaei et al., 2008; Lucas et al., 2003; Parsapoor et al., 2008; 2012a; 2012b].

The organization of this paper is as follows: first, a brief review of related works in modelling of brain emotional learning is given in Section 2. The suggested BELRFS model is described in more detail in Section 3. Solar activity and geomagnetic storm forecasting are examined using the BELRFS and the result is compared to LoLiMoT, in Section 4. Finally, we conclude this paper by reviewing the main results and adding some remarks about the performance of BELRFS and also we suggest some ideas for future extension of BELRFS in Section 5.

2 BACKGROUND

For a long time, emotion was not assumed to be related to intelligence in human beings [Custodio et al., 1999]. Hence, the emotional aspect of human behaviour has so far received somewhat limited attention in the artificial intelligence research fields. In 1988 emotion was first proposed to be a principle part in human reaction [Fellous et al., 2003]. Since that time, neuroscientists have started to conduct experimental studies to explore emotion-based behaviours and analyze emotional processing. The studies have led to the explanation of emotional reactions by the application of different psychological theories, e.g., central theory and cognitive theory [Fellous et al., 2003]. Another contribution of these studies was the development of computational models of emotional learning that have been used to develop artificial intelligence (AI) tools, intelligent controller [Lucas et al., 2004; Zadeh et al., 2006 Custodio et al., 1999] and data driven prediction methodologies [Babaei et al., 2008; Lucas et al., 2003; Parsapoor et al., 2008; 2012a; 2012b]. A good example of the computational models is a model that has been proposed on the basis of central theory and aims to model emotional learning and memory [Fellous et al., 2003]. The amygdala-orbitofrontal subsystem that was proposed, based on the internal structure of emotional system and central theory is another computational model [Moren et al.,2000;2002; Balkenius, et al., 2001].

2.1 Anatomical Aspects of Emotional Learning

Numerous studies have been conducted to reveal the anatomical, hormonal and behavioral aspects of emotional learning. These studies have proven that the limbic system in mammalian brains has the main responsibility for emotional learning [Reisbetg et al., 2009; Gazzaniga et al., 2009; Arbib 2002; Fellous et al., 2003]. The limbic system contains several regions, these regions are: the hippocampus, the amygdala, the thalamus and the sensory cortex. The role of each region in the context of emotional learning (fear conditioning and classical conditioning) is summarized as follows:

1) *Thalamus* is responsible for the provisioning of high-level information about the received emotional stimuli [Moren et al., 2000; Balkenius, et al., 2001; 2002].

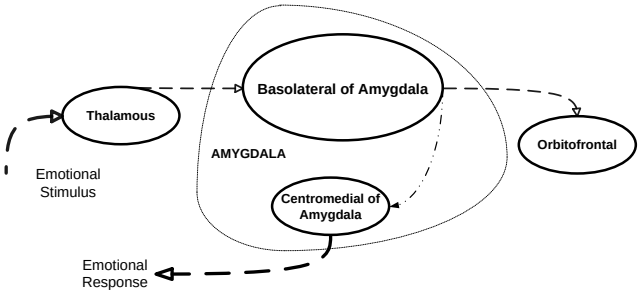

Figure 1 *The pathways between the parts of the limbic system have a role in emotional learning.*

2) *Sensory cortex* is responsible to analyze the received signal from the thalamus and distribute the signal between the amygdala and the orbitofrontal regions [Moren et al., 2000; Balkenius, et al., 2001; 2002].

3) *Amygdala* is the central part of the limbic system and has a main role in emotional learning [Moren et al., 2000; Balkenius, et al., 2001; 2002]; it has direct connections with thalamus, sensory cortex and orbitofrontal (that is located at the front of the brain) (see Figure 1) [Jenkins et al., 1998; Ferry et al., 1999;Moren et al., 2000; Balkenius, et al., 2001; 2002; Hooker et al., 2006]. It participates in storing emotional experiences and emotional responses [Hooker et al., 2006], evaluating positive and negative reinforcement and emotional reactions [Ferry et al., 1999], learning and predicting the association between unconditioned and conditioned stimuli [Ferry et al., 1999]. It encompasses two main parts: basolateral complex and centromedial nucleus [Best 1992; Kandel et al., 2003]. The basolateral complex is the largest part of the amygdala and performs the role of mediating memory consolidation [Reisbetg et al., 2009]. It not only passes stimuli to other parts of the amygdala, but also forms the stimulus-response association [Ferry et al., 1999]. The second part centromedial nucleus that encompasses the medial nucleus and the central nucleus has a role in mediating the expression of emotional responses [Kandel et al., 2003; Reisbetg et al., 2009].

4) *Orbitofrontal cortex* is located close to the amygdala and has a bidirectional connection to the amygdala. This part is involved in processing the stimuli, learning the stimulus–reinforcement association. It also evaluates the reinforcement signal to prevent the amygdala from providing an inappropriate response [Moren et al., 2000; Balkenius, et al., 2001; 2002].

2.2 Mathematical Aspects of Emotional Learning

An essential step in developing a computational model of emotional learning is representing emotional processing, using mathematical equations. One well-known computational model of emotional learning is the Amygdala-orbitofrontal subsystem model [Moren et al.,

2000; Balkenius, et al., 2001; 2002]. It was developed on the basis of the internal structure of the limbic system, specifically the amygdala and its connections. The Cathexis model [Velásquez 1998] was inspired by human decision-making process; it was essentially based on a combination of basic neuropsychological and ethological theories and imitates the internal structure of emotional processing, specifically the prefrontal lobe and its connections. The hippocampus-neocortex model [Kuremoto et al., 2009a] was a modified model of the conventional model of the hippocampus; it aims at increasing the capability of processing plural time-series by adopting a multilayer chaotic neural network. The amygdala hippocampus model [Kuremoto et al., 2009a] proposed a combination between associative memory and emotional learning to improve the hippocampus-neocortex model [Kuremoto et al., 2009b]. Later, a model of the limbic system [Kuremoto et al., 2009b] was proposed as an enhancement of the two previous models. Reversal emotional learning [Hattan et al., 2012] was developed on the basis of the hormonal aspects of emotional learning to simulate food seeking behavior. Model of mind [Zadeh et al., 2006] was introduced as a modular model to imitate emotional behavior; a goal based agent was implemented on the basis of this model. This agent has an efficient ability to react to changes in the environment.

The amygdala-orbitofrontal subsystem model has inherited its structure from the limbic system. It structure imitates the connection between those parts of the limbic system that have a role in emotional learning. The amygdala-orbitofrontal subsystem consists of four parts which interact with each other to form the association between the conditioned and the unconditioned stimuli (see fig. 2). [Moren et al., 2000; Balkenius, et al., 2001; 2002]. In this model, the orbitofrontal and amygdala are represented by several nodes with linear functions. The nodes' output of the amygdala and the orbitofrontal cortex are referred to as $\boldsymbol{A}$ and $\boldsymbol{O}$, respectively. The output of the model is represented as $\boldsymbol{E}$ and is formulated as equation (1).

$$\mathbf{E} = \sum_i A_i - \sum_i O_i \tag{1}$$

The updating rules of the model are based on $\boldsymbol{A}$, $\boldsymbol{O}$ and the reinforcement signal $\boldsymbol{REW}$. The updating rules are formalized as equations (2) and (3) and are utilized to adjust the weights. These weights V_i and W_i are associated to the nodes of the amygdala and orbitofrontal subsystem, respectively [Moren et al., 2000; 2002; Balkenius, et al., 2001]. Here S_i is the input of i th node of amygdala and orbitofrontal.

$$\Delta V_i = \alpha(S_i \times \max(0, \mathbf{REW} - \sum_j A_j)) \tag{2}$$

$$\Delta W_i = \beta(S_i \times (\sum_j O_j - \mathbf{REW})) \tag{3}$$

The basic amygdala-orbitofrontal subsystem model has a simple structure and can be used as a foundation for new computational-models. Furthermore, machine learning techniques can be developed based on such models. In the next subsection, some emotionally-based machine learning methods based on the amygdala-orbitofrontal subsystem are described.

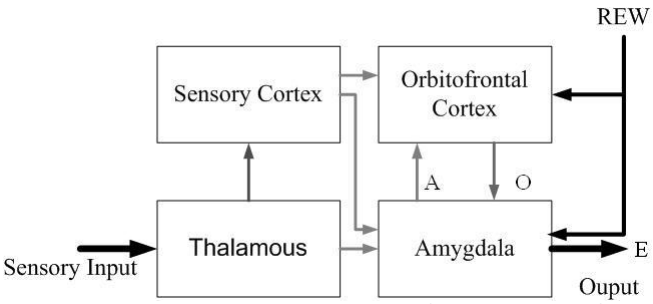

Figure 2 *The graphical description of amygdala-orbitofrontal subsystem.*

2.3 Brain Emotional Learning-based Methodologies

The Brain Emotional Learning Based Intelligent Controller (BELBIC) [Lucas et al., 2004] can be considered as the first practical implementation of an emotionally-inspired controller. BELBIC was developed on the basis of Moren and Balkenius' computational model [Lucas et al., 2004;]; it has been successfully applied for a number of applications: controlling heating and air conditioning [Sheikholeslami, et al., 2005], aerospace launch vehicles [Mehrabian, et al., 2006], and intelligent washing machines [Milasi, et al., 2005]. BELBIC, that is an emotionally-inspired controller, has the ability to overcome the uncertainty and complexity issues of classic controller models. Studies [Lucas et al., 2004; Sheikholeslami et al., 2005; Milasi et al., 2005; Mehrabian et al., 2006] have also proved that the BELBIC outperforms many other models such as PID controllers and linear controllers in terms of simplicity, reliability and stability.

Other types of brain emotional learning-based model are Emotional Learning based Fuzzy Inference System (ELFIS) [Lucas et al., 2004], Brain Emotional Learning (BEL) [Babaei et al., 2008], Recurrent Reinforcement Fuzzy inference system based Brain Emotional Learning (RRFBEL), BELRFS and Brain Emotional Learning based Fuzzy Inference System (BELFIS) [Parsapoor et al., 2008; 2012a, 2012b]; they have also been developed for prediction applications. The mentioned models are based on different structures and functions than the amygdala-orbitofrontal subsystem and have been shown to enhance the prediction accuracy, particularly for chaotic prediction applications [Lucas et al., 2003; Golipour et al., 2004; Parsapoor et al., 2008; Parsapoor et al., 2012].

3 BRAIN EMOTIONAL LEARNING BASED RECURRENT FUZZY SYSTEM (BELRFS)

In this section, we explain the structure, function and the learning algorithm of BELRFS. We illustrate how the model is divided into different parts trying to mimic the structure of the emotional network. We also explain the functionality of the model using adaptive neuro-fuzzy networks. Finally, the learning algorithm and the updating rules of BELRFS are given.

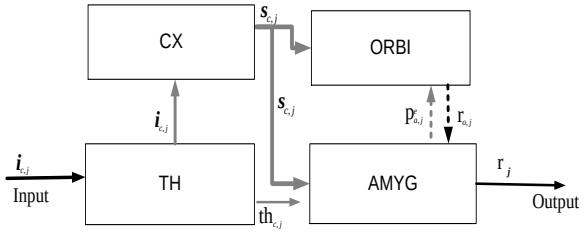

Figure 3 *The connection between the parts of BELRFS.*

3.1 Model Description

Similar to the amygdala-orbitofrontal model, BELRFS model consists of four main parts, which are referred to as THalamous, sensory CorteX, AMYGdala and ORBItofrontal cortex, and are named as TH, CX, AMYG and ORBI, respectively. Figure 3 describes the structure of BELRFS when it is faced with an input vector from the training data samples. Assuming $\mathbf{i}_{u,j}$ is an input vector of the set of training samples, $\mathbf{I}_u = \{\mathbf{i}_{u,1}, \mathbf{i}_{u,2}, ..., \mathbf{i}_{u,N_u}\}$ where the subscripts u and j indicate that the sample is j^{th} vector of training samples; while, N_u determines the number of training samples, the structure and the function of each part are illustrated as follows:

1) *TH* has connections with the CX and the AMYG and it is subdivided into two units: the MAX (MAXimum unit) and the AGG (AGGregation unit). The TH is where that the input vector, $\mathbf{i}_{u,j}$, enters to the BELRFS. The function of the MAX is described by the competitive neural network as equation (4). Assuming $\mathbf{i}_{u,j}$ is a vector with m dimensions $\mathbf{i}_{u,j} = [i_{u,j,1}, i_{u,j,2}, ..., i_{u,j,m}]$, equation (4) determines the maximum value of $\mathbf{i}_{u,j}$. The AGG unit consists of a pre-trained neural network with linear nodes; it receives $\mathbf{i}_{u,j}$ and passes to the CX.

$$\mathbf{th}_{u,j} = [\max(\mathbf{i}_{u,j})] \tag{4}$$

2) *CX* has connections with AMYG, ORBI and TH. The CX imitates the function of the sensory cortex using a pre-trained single layer linear neural network. The CX provides, $\mathbf{s}_{u,j}$ that is sent to both AMYG and ORBI. It should be noted that $\mathbf{i}_{u,j}$ and $\mathbf{s}_{u,j}$ have the same entity; however they are originated at different parts.

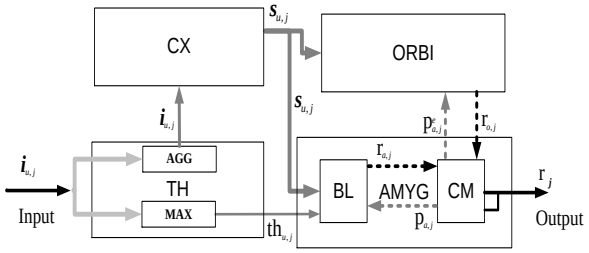

Figure 4. *The structure of BELRFS and its connections.*

3) *AMYG* has connections with all other parts. It receives two inputs, $\mathbf{th}_{u,j}$ and $\mathbf{s}_{u,j}$, which are originated from TH and the CX, respectively. As Figure 4 depicts, the AMYG is divided into two units: BasoLateral (BL) and CentroMedial (CM); they imitate the functionality of the basolateral complex and the centromedial nucleus, respectively. Using an adaptive neuro-fuzzy network, the function of BL can be described as equation (5). Here, F is a fuzzy function according to equation (20). The provided output of BL, $r_{a,j}$, is considered as the primary response of the BELRFS.

$$r_{a,j} = \mathrm{F}([s_{u,j}, th_{u,j}]) \tag{5}$$

The primary response, $r_{a,j}$, is sent to CM, where the final output of BELRFS, r_j, is produced in accordance with equation (6). In CM, the output of the recurrent adaptive neuro-fuzzy network, which is the main part of CM, is the final output of the BELRFS. Here, REW_j indicates the recurrent signal that can be defined as equation (7).

$$r_j = \mathrm{F}([r_{a,j}, r_{o,j}, REW_j]) \tag{6}$$

$$REW_j = 1 - \mathrm{G}(r_j, r_{u,j}) \tag{7}$$

The function G is calculated as (8).

$$\mathrm{G}(r_j, r_{u,j}) = (r_j(t-1) - r_{u,j}(t-1)) + \frac{\sum_{j=1}^{N}(r_j(t-2) - r_{u,j}(t-2))^2 + \sum_{j=1}^{N}(r_j(t-1) - r_{u,j}(t-1))^2}{\sum_{j=1}^{N}(r_{u,j} - \bar{r}_{u,j})^2} \tag{8}$$

Other components of CM are two square nodes with the summation functions to provide the reinforcement signals, $p^e_{a,j}$ and $p_{a,j}$. The former, $p^e_{a,j}$, represents the expected reinforcement signal and is formulated by equation (9).

$$p^e_{a,j} = \lambda_a r_{a,j} + \lambda_u r_{u,j} \tag{9}$$

Where $r_{u,j}$ ($r_u = \{r_{u,1}, r_{u,2}, ...\}$) is the correspondent output value to $i_{u,j}$. The λ_a and λ_u are two values from $\boldsymbol{\lambda} = \lambda_a, \lambda_o, \lambda_b, \lambda_u$ that is the set of weights. The parameter $p_{a,j}$ is the reinforcement signal that is provided by the CM as an estimation of the ORBI's response. When CM receives the provided response from ORBI, it evaluates it ($r_{o,j}$) and provides a reinforcement signal as $p_{a,j}$ and sends it to the ORBI.

4) ORBI receives $\mathbf{s}_{u,j}$ from CX and $p^e_{a,j}$ from CM and sends the response, $r_{o,j}$ back to the CM. This response is considered as the secondary response. In fact, the ORBI, forms the input-reinforcement mapping using a feed forward adaptive neuro-fuzzy network. The function of the ORBI is defined by equation (9). Here, F is a fuzzy function according to equation (10).

$$r_{o,j} = \mathrm{F}([s_{c,j}]) \tag{10}$$

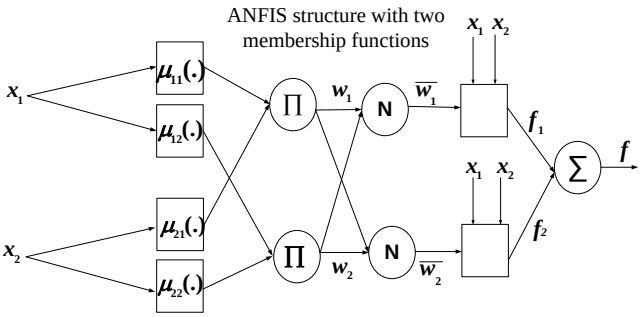

Figure 5 *A simple adaptive network with two input and two membership function for each inputs.*

It should be noted that the structure of CM differs during the training phase and the test phase. When it is faced by inputs from the training set, a recurrent signal is returned to the CM. However, during the test phase, the recurrent signal is removed and the REW_j is calculated using weighted k-nearest neighbor method.

As mentioned earlier, the BELRFS mimics the emotional conditioning process and learns the input-output mapping according to the stimulus-emotional response association.. The TH and the CX are defined by using very simple neural networks. In contrast, we adapt feed forward and recurrent adaptive neuro-fuzzy networksfor the AMYG and ORBI. In the next subsection, we explain the structure and function of an adaptive neuro-fuzzy network emphasizing the recurrent adaptive network.

3.2 Recurrent Adaptive Neuro-fuzzy Network

An adaptive neuro-fuzzy network is a type of fuzzy inference system which is structurally defined by an adaptive network. This type of network consists of five layers where each layer has some adaptive nodes (circular and square nodes). The circular nodes are fixed nodes and have no parameters. The square nodes, fully adaptive nodes, might have different functions and different parameters. The main characteristic of the adaptive network is that the feed forward links only show the direction of inputs to nodes and outputs of nodes, these links do not have any associated weights [Jang et al., 1997]. Figure 5 displays an adaptive neuro-fuzzy network with a two dimensional input vector. Using the Sugeno fuzzy inference system, it can be defined as equations (10) and (11).

If x_1 is μ_{11} and x_2 is μ_{12} then $f_1 = q_{11}x_1 + q_{12}x_2 + q_{13}$ (10)

If x_1 is μ_{21} and x_2 is μ_{22} then $f_1 = q_{11}x_1 + q_{12}x_2 + q_{13}$ (11)

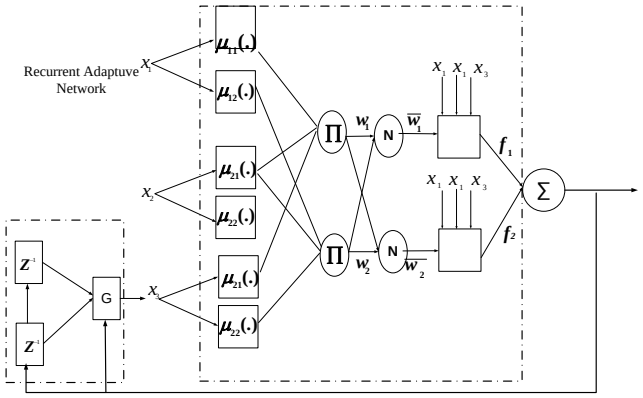

Figure 6 *Recurrent adaptive network.*

If there is a feedback link, then the adaptive network is recurrent. As a matter of fact, a recurrent adaptive network consists of feed forward layers with circular and square nodesand a recurrent layer with some delay nodes and square nodes to produce the recurrent signal (see Figure 6). Figure 6 depicts the recurrent adaptive network that can be expressed using Sugeno and Tsukomoto fuzzy inference as equations (12) and (13). These equations explain a very simple Sugeno fuzzy inference system with two rules.

If x_1 is μ_{11} and x_2 is μ_{12} and x_3 is μ_{13} then

$$f_1 = q_{11}x_1 + q_{12}x_2 + q_{13}x_3 + q_{14} \quad (12)$$

If x_1 is μ_{12} and x_2 is μ_{22} and x_3 is μ_{23} then

$$f_2 = q_{12}x_1 + q_{22}x_2 + q_{23}x_3 + q_{24} \quad (13)$$

The following steps explain the function of each layer of this network considering two membership functions for each input. The input vector consists of $\mathbf{x} = x_1, x_2, x_3$. Where x_3 is equal to the recurrent signal.

Layer 1: It consists of square nodes with Gaussian or Bell-shaped functions which can be defined by equations (14) and (15), respectively.

$$\mu_j(x_j) = exp(-\frac{1}{2}\frac{(x_j - c_j)^2}{\sigma_j^2}) \quad (14)$$

$$\mu_{ij}(x_j) = \frac{1}{1+\left|\frac{x_j - c_{ij}}{a_{ij}}\right|^{2b_{ij}}} \quad (15)$$

Where x_j is the j^{th} dimension of an n dimensional input vector. And $\{a_{ij}, b_{ij}, c_{ij}\}$ is the set of parameters of the membership function. Here l specifies that this membership function is l^{th} membership function of x_j .

Layer 2: It consists of the circular nodes which are labeled with $\prod$ *and* calculates the multiplication of the inputs as equation (17).

$$w_l = \prod_{j=1}^{n} \mu_{lj}(x_j) \quad (17)$$

Layer 3: It consists of circular nodes which are labeled with $\overline{\mathrm{N}}$; the output of the $\overline{\mathrm{N}}$ node is defined as equation (18), where m determines the number of fuzzy rules that is equal to the number of circular nodes of layer 2.

$$\overline{w_l} = \frac{w_l}{\sum_{l=1}^{m} w_l} \tag{18}$$

Layer 4: It consists of square nodes to provide the *then* part of the Sugeno fuzzy rules using (19).

$$\mathrm{f}_l = \sum_{j=1}^{n} q_{lj} x_j + q_{l(j+1)} \tag{19}$$

Layer 5*:* It consists of a summation node and provides the final output of adaptive network as (20) [29].

$$\mathrm{F}(\mathbf{x}) = \sum_{l=1}^{m} \overline{w}_l \, \mathrm{f}_l(\mathbf{x}) \tag{20}$$

The subscript l shows the output of l^{th} fuzzy rules of fuzzy rules, $\mathbf{X}$ indicates an input vector and $\overline{w}_l$ is calculated using equation (18).

Layer 6: It consists of a recurrent layer and includes a set of unit-delay nodes (in this case are two unit-delay nodes included) to provide a feedback of the final output. This layer also has a square node with G function to feed the provided feed back to the first layer(see x_3 in Figure 6).
It should be noted that the described recurrent adaptive network is similar to the feed forward type; however we have defined the 6th layer with a set of unit-delay nodes and feedback signal.

3.2 Weighted KK Nearest-Neighbour

As was mentioned earlier, for unseen input from the test set, the value of $\mathbf{REW}_{test}$ is estimated using the weighted k nearest neighbor (W-kNN). The following steps explain how $\mathbf{REW}_{test}$ is calculated using WKNN:

1) For each $\mathbf{i}_{tset}$, the Euclidean distance $d_j = \left\| \mathbf{i}_{test} - \mathbf{i}_{u,j} \right\|_2$ is calculated, where $\mathbf{i}_{u,j}$ is a member of the training data set $\{\mathbf{i}_{u,1}, \mathbf{i}_{u,2}, ..., \mathbf{i}_{u,N_u}\}$.

2) For each test sample, e.g., $\mathbf{i}_{tset}$, a subset of k minimum values of $\mathbf{d} = \{d_1, d_2, ..., d_{N_u}\}$ is selected and referred to as as $\mathbf{d}_{\min}$. It is a set that is corresponding to the k nearest neighbors of the test sample.

3) For these neighbors, a subset of $\mathbf{REW} = \{REW_1, ..., REW_{N_u}\}$ is selected and this subset is referred to as $\mathbf{REW}_{\min}$.

4) For the test sample, $\mathbf{i}_{tset}$, the value of REW_{test} is determined as equation (21).

$$REW_{test} = \left(\sum_{j=1}^{k} v_j \times REW_{u,j} \Big/ \sum_{j=1}^{k} v_j\right) \tag{21}$$

Where, w_j, is calculated as the kernel equation (22).

$$v_j = \mathrm{K}(d_j) \tag{22}$$

The kernel function K(.) converts Euclidian distances to the weights according to equation (23).

$$\mathrm{K}(d) = \frac{\max(\mathbf{d}) - (d_j - \min(\mathbf{d}))}{\max(\mathbf{d})} \tag{23}$$

3.3 Learning Algorithm

The BELRFS model learns the input-output mapping using local learning algorithms were the learning parameters of the adaptive networks are independently adjust. In other words, the linear and nonlinear parameters of each adaptive network are updated using the hybrid learning algorithm that was given by [Jang et al., 1997].

For updating the nonlinear parameters, each adaptive network uses the steepest descent (SD) algorithm to minimize its loss function. The loss functions are converged to minimum values using the SD for updating all nonlinear learning parameters.

The overall loss function can be defined as equation (13); choosing appropriate values for $\boldsymbol{\lambda}$ ($\boldsymbol{\lambda} = \lambda_a, \lambda_o, \lambda_b, \lambda_u$), the loss function, $lossfun$, of each adaptive network can be derived by equation (24)

$$lossfun = (\lambda_a r_{a,j} + \lambda_o r_{o,j} + \lambda_b r_j + \lambda_u r_{u,j})^2 \tag{24}$$

For the adaptive network of BL, the $\boldsymbol{\lambda}$ vector is defined as $\boldsymbol{\lambda} = \lambda_a, 0, 0, \lambda_u$ and the loss function is defined as equation (25). While, the loss function for updating the nonlinear parameters of ORBI is defined as equation (26).

$$lossfun_{BL} = (\lambda_a r_{a,j} + \lambda_u r_{u,j})^2 \tag{25}$$

$$lossfun_{ORBI} = (\lambda_a r_{a,j} + \lambda_o r_{o,j} + \lambda_u r_{u,j})^2 \tag{26}$$

For updating the linear parameters, an offline version of Least Squares Estimate (LSE) is used under the assumption that the nonlinear parameters have been updated and their values are fixed.
Let us assume $\{\mathbf{x}_j\}_{j=1}^{N_u}$ as inputs of the adaptive network of BL, the output can be represented as $\mathbf{r}_a = \{r_{aj}\}_{j=1}^{N_u}$. Equation (27) formulates the output of the BL.

$$r_{aj} = \sum_{l=1}^{m} \overline{w}_l (x_{1j} q_{1l} + x_{2j} q_{2l} + q_{3l}) \tag{27}$$

Consideringthat each pair of the set $(\mathbf{x}_j, r_{a,j}), j = 1,...N_u$ is substituted into equation (27), then, N_u linear equations are provided; these equations can be rewritten in a matrix-form as equation (28).

$$\mathbf{A} = \left[\bar{w}_{11}x_{1j}, \bar{w}_{11}x_{2j}, \bar{w}_{11}, ..., \bar{w}_{1m}x_{1j}, \bar{w}_{1m}x_{2j}, \bar{w}_{1m}\right]_{j=1}^{N_u} \quad (28)$$

Thus, the linear parameter can be calculated as equation (29).

$$\mathbf{q}_a = (\mathbf{A}^{\mathrm{T}}\mathbf{A})^{-1}\mathbf{A}^{\mathrm{T}}\mathbf{r}_a \quad (29)$$

The linear parameters of CM and ORBI is calculated repeating the above steps. During the learning phase, the learning parameters, linear and nonlinear, can be updated by using one of the methods below:

1. All parameters can be updated using the steepest descent.
2. The nonlinear parameters are updated using steepest descent and LSE are applied to update the linear parameters.

Certainly, these methods differ in terms of time complexity and prediction accuracy and a trade-off between high accuracy and low computational time must be considered to choose a feasible method.

4 PREDICTION CHAOTIC TIME SERIS

In [Parsapoor et al., 2012], the long term prediction of two chaotic time series, Lorenz and Ikeda were investigated by applying BELRFS and LoLiMoT. The obtained results showed a fairly good performance of BELRFS in long term prediction. In this paper, BELRFS is applied both for long term and short term prediction of three benchmark time series: Lorenz, sunspot time series and Auroral Electrojet (AE) index. The result of applying BELRFS is compared with previous results using local linear neuro-fuzzy models with linear model tree algorithm (LoLiMoT), which is a well-known neuro-fuzzy method. To evaluate the prediction performance, we use the Normalized Mean Square Error index (NMSE) and Normalized Root Mean Square Error (NRMSE) that are calculated according to equations (30) and (31), respectively.

$$NMSE = \frac{\sum_{j=1}^{N}(Y_j - \hat{Y}_j)^2}{\sum_{j=1}^{N}(Y_j - \bar{Y}_j)^2} \quad (30)$$

$$NRMSE = \sqrt{\frac{\sum_{j=1}^{N}(Y_j - \hat{Y}_j)^2}{\sum_{j=1}^{N}(Y_j - \bar{Y}_j)^2}} \quad (31)$$

Where $\hat{Y}$ and Y refer to the observed values and the desired targets, respectively; and $\bar{Y}$ is the average of desired targets.

4.1 Prediction of Lorenz Chaotic Time series

Lorenz time series is a well-known benchmark chaotic time series and has been tested for long-term and short term prediction by different methods, e.g., neural network and neuro-fuzzy methods [Golipour et al., 2006a; 2006b], [Chandra et al., 2012]. In this section, both long-term and short term predictions of Lorenz time series are examined for BELRFS and LoLiMoT. The Lorenz time series is reconstructed by equation (32). Using equation (33), we assigned the standard values that has been defined by Lorenz [Rasband 1990]. The ratio of sampling to reconstruct the time series is considered as 0.01 seconds. The initial values are considered as $x = -15, y = 0, z = 0$ [Golipour et al., 2006a; 2006b].

$$\begin{aligned} \dot{x} &= a(y - x) \\ \dot{y} &= bx - y - xz \\ \dot{z} &= xy - cz \end{aligned} \quad (32)$$

$$a = 10, b = 28, c = 8/3, T = 0.01s \quad (33)$$

As a first experiment, short term and long term prediction of the Lorenz time series aretested by BELRFS. For this purpose, the data samples from the 30th second to 55th second are selected; the first 1500 samples are considered as the training data samples and the remaining samples are chosen as the test samples. It should be noted that the embedded dimension of reconstructed time series is selected as three. Table I presents the obtained NMSEs by applying BELRFS and LoLiMoT for predicting one step ahead, ten and twenty steps ahead of the Lorenz time series. The predicted values versus the observed values are depicted in Figure 7.

BELRFS is also employed for multi-step prediction (ten steps ahead and twenty steps ahead) for the similar data set of Lorenz. Table I lists the NMSEs for multi-step ahead predictions which are achieved by LoLiMoT and BELRFS. As Table I indicates, the BELRFS has the capability to achieve highly accurate results for both short and long term prediction of chaotic time series.

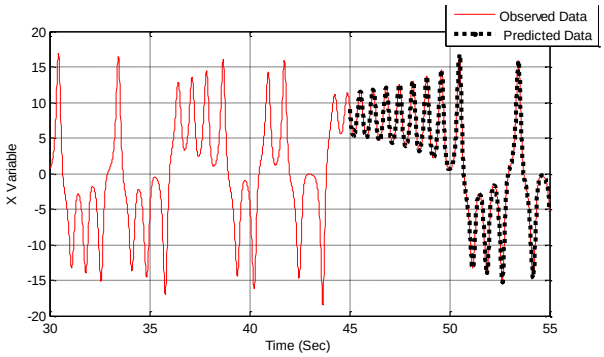

Figure 7. The predicted value of one step ahead prediction of Lorenz time series by applying BELRFS.

TABLE I. THE NMSES OF BELRFS AND LOLIMOT TO PREDICT MULTI-STEP AHEAD OF LORENZ TIME SERIS

Learning Model	NMSE index for multi-step ahead prediction		
	1 step ahead	*10 step ahead*	*20 step ahead*
BELRFS	4.85e-10	2.72e-6	0.0017
LoLiMoT	9.81e-10[Golipour et al., 2006a]	0.0011	0.0442

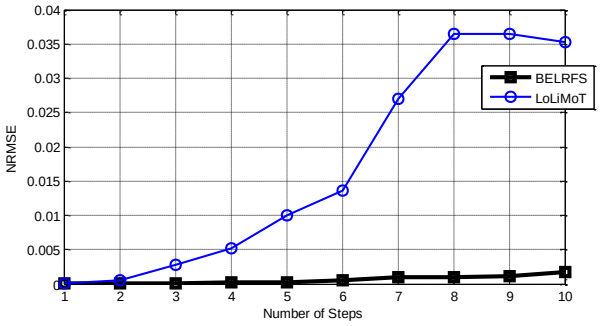

(a)

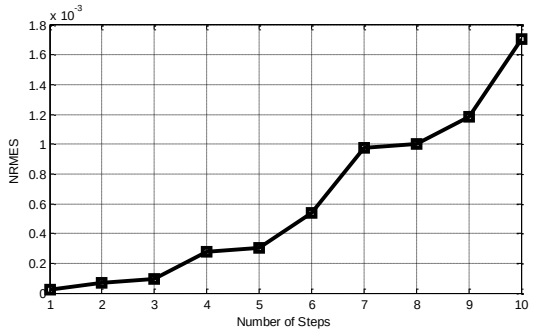

(b)

Figure 8. The NMRSE of BELRFS and LoLiMoT for multi-step ahead prediction.

Figure 8 shows the NRMSEs that are obtained from using BELRFS and LoLiMoT for multi-step ahead prediction of Lorenz time series. For short term prediction the NRMSE of BELRFS and LoLiMoT are approximately equal; while for long term prediction, the NRMSE of BELRFS is much lower than for LoLiMoT(see Figure 8. (a)). Figure 8. (b) Indicates how NRMSEs increase with the raise in prediction steps.

As mentioned earlier, the Lorenz chaotic time series is a well-known benchmark time series and has been tested with a numerous data-driven models to evaluate its performance.

Table II includes the obtained NMSEs of several data-driven methods: Nonlinear Autoregressive model with eXogenous input (Hybrid NARX-Elman RNN) [Chandra et al., 2012], Evolving Recurrent Neural Networks(ERNN) [Ma et al., 2007], Radial Basis Function (RBF), multilayer perceptron (MLP) [Golipour et al., 2006a], Support Vector Regression(SVR),Tapped Delay Line Multilayer Perceptron(TDL_MLP),Distrbuted Local Experts based on Vector_Quantization using Information Theoretic learning (DLE_VQIT))[Martinez et al.,2008], Cooperative Coevolution of Elman Recurrent Neural Networks (CCRNN) [Chandra et al., 2012]. Table II indicates that for short-term prediction of chaotic time series, the BELRFS outperforms most of the data driven models in term of prediction accuracy. Only Hybrid NARX-Elman RNN methodhas less NMSE than BELRFS. The NMSE of this method is equal to 1.98e-10 that is less than the NMSE of BELRFS, see Table II.

To further evaluate the performance of the BELRFS and verify its robustness, white noise with standard deviation 0.1 is added to the first data set. Table III lists the obtained results of applying BELRFS and the results of other methods: Recurrent Neural Network trained with Real-time Recurrent Learning (RNN_RTRL), Recurrent Neural Network trained with the second-order extended Kalman filter (RNN_EKF), Recurrent Neural Network trained with the algorithm and backpropagation through time (BPTT) , feedforward Multi layer Perceptron trained with the Bayesian Levenberg–Marquardt (MLP-BLM), recursive second-order training of recurrent networks via a recursive Bayesian Levenberg–Marquardt (RBLM-RNN) algorithm. It is noticeable that the NMSE of BELRFS for predicting noisy data samples with 0.1standared variation is lower than most of listed methods.

TABLE II. THE NMSES OF DIFFERENT METHODS TO PREDICT MULTI-STEP AHEAD OF LORENZ TIME SERIS

Learning Model	Specification		
	NMSE	***Time series***	***No. Training Test data***
NARX [Ardalani et al.,2010]	1.9e-10	One step ahead	1500,1000
BELRFS	***4.9e-10***	***One step ahead***	***1500,1000***
ERNN [Ma et al., 2007]	9.9e-10	One step ahead	1400,1000
RBF [Golipour et al., 2006a]	1.4e-9	One step ahead	1500,1000
MLP [Golipour et al., 2006a]	5.2e-8	One step ahead	1500,1000
CCRNN	7.7e-4	Two steps ahead	500,500
SVR [Martinez et al., 2008]	1.5e-2	One step ahead	----
TDL_MLP [Martinez et al., 2008]	1.6e-4	One step ahead	----
DLE_VQIT [Martinez et al., 2008]	2.6e-4	One step ahead	----

TABLE III. DIFFERENT METHODS FOR MULTI_STEP AHEAD OF NOISY LORENZ DATA.

Method	Specifications		
	NMSE	***Time series***	***No. Training Test data***
BELRFS	***5.7e-4***	***One step ahead of noisy data (STD 0.1)***	***1500,1000***
LNF-LSSVMs [Miranian et al., 2013]	4.4e-4	One step ahead of noisy data (STD 0.05)	1000,250
RBLM-RNN [Mirikitani et al 2010]	6.8e-4	One step ahead of noisy data (STD 0.05)	1000,250
RNN-EKF [Mirikitani et al 2010]	7.2e-4	One step ahead of noisy data (STD 0.05)	1000,250
LLNF with LoLiMoT algorithm [Miranian et al., 2013]	7.7e-4	One step ahead of noisy data (STD 0.05)	1000,250
MLP_BLM [Mirikitani et al 2010]	8.1e-4	One step ahead of noisy data (STD 0.05)	1000,250
RNN_BPTT [Mirikitani et al 2010]	1.1e-3	One step ahead of noisy data (STD 0.05)	1000,250
RNN_RTRL [Mirikitani et al 2010]	1.0e-3	One step ahead of noisy data (STD 0.05)	1000,250

4.3 Forecasting Space Weather Storms

Recently, monitoring and forecasting of space weather storms with AI algorithms have received a lot of attention. As an example, 'Lund Space Weather Model' [Lundstedt et al., 2002] was a type of AI-based models that has been applied to predict the space weather and its harmful impacts on space-based equipment [Lundstedt et al., 2002]. Space weather storms and short-term variations in the Earth's external magnetic field have harmful effects on various systems, e.g. Global Positioning System (GPS), space-ground communications and electrical power networks. One of the objectives of forecasting space weather is to reduce or prevent the damaging effects of space storms on electrical and telecommunication equipment.

The Sun and the solar wind have been known as the main sources of space weather storms. Powerful magnetic forces on the Sun's surface induce regional temperature variations on the Sun's surface. These spatial temperature variations are the main origin of solar activity, which has a periodic characteristic named the solar cycle. One cycle consists of a solar maximum and a solar minimum. Both of them are determined based on the number of sunspots on the Sun's surface. During the solar maximum, the number of sunspots increases; it shows a rise in solar activity. Thus, the number of sunspots and the time series driven by sunspots can be utilized to forecast solar activity and its harmful effects (solar storms) [Lundstedt et al., 2002; Golipour et al., 2004; 2006a; 2006b]. So far, MLP, RBF and recurrent neural networks (RRN) have been applied to predict sunspot number time series in order to forecast space storms [Lundstedt et al., 2002].

Other sources of space weather storms are the solar wind and the Earth's magnetosphere that have a major effect on geomagnetic activities. It has been shown that the expansion and the strength of the auroral electrojet is influenced by geomagnetic activities. Hence, the Auroral Elecrtrojet index (AE index) is suggested as one of quantitative measures of geomagnetic activities [Davis et al., 1965]. Its driven time series is a reliable time series for space storm prediction[Golipour et al., 2006a; Babaie et al., 2008] Due to the complex dynamic nature of auroral electrojet activity, the nature of AE index and its driven time series are also chaotic . Thus, the accurate prediction of the AE index, which is crucial in order to predict geomagnetic storms, is not easily achievable. The chaos degree of AE time series [Golipour et al., 2006a] indicate that it is predictable for short-term prediction, e.g. one minute ahead prediction [Golipour et al., 2006a; Babaie et al., 2008]; while achieving highly accurate results for long-term prediction of the AE is almost impossible. In light of this fact, data approach methods such as neural networks and neuro- fuzzy methods, [Babaie et al., 2008] even emotion-learning methods, have been applied for short-term and long-term prediction of the AE index.

4.3.1 Forecasting Solar Activity

As was mentioned earlier, sunspot time series is a good measure of solar activity. Different techniques have been utilized for forecasting solar activity using the sunspot numbers. Data driven approaches, e.g., linear and nonlinear autoregressive methods,, neural networks (MPL and RFB) and neuro-fuzzy methods (ANFIS and LoLiMoT) and even emotionally-based machine learning methods (ELFIS, RRFBEL, BEL, BELFIS,BELRFS) have been applied to predict solar activity [Lundstedt et al., 2002; Golipour et al., 2004; 2006a; 2006b; Parsapoor et al., 2008]. The conducted studies have verified that neural networks and neuro-fuzzy methods have the high capability to model (predict) the dynamic behavior of sunspots. The issue of neural networks is that they require a large number of data samples to learn the chaotic and nonlinearity behavior of dynamic time series [Lucas et al., 2003; Golipour et al., 2004;2006 a; 2006 b] andneuro-fuzzy methods suffer from the curse of dimensionality. The results of performed studies based on emotional learning [Golipour et al., 2004; Parsapoor et al., 2008; Lucas et al., 2003] indicate that these models have the capability to achieve more accurate results than neuro-fuzzy and neural networks [Golipour et al., 2004; Parsapoor et al., 2008; Lucas et al., 2003]. Thus, it is still interesting to apply new emotional based learning models for solar activity forecasting. For this purpose, BELRFS is applied to predict sunspot number time series. As a first experiment a non-smoothed monthly sunspots time series, a part of solar cycle 19, is selected to be as an experiment comparing the prediction abilities of BELRFS and LOLIMOT. The solar cycle 19 started in 1954 and ended in 1964; we test the set containing the sunspots from 1950 to 1965. This set includes the peak sunspot number of solar cycle 19, which occurred in 1957. The obtained results of applying BELRFS, LOLIMOT and their specifications are listed in Table IV. Figure 9 shows the predicted value by BELRFS.

It can be seen that BELRFS predicts the peak value as 238 that is close to the observed value of the peak point, in 1957. In comparison with LoLiMoT, BELRFS has a little bit higher NMSE than LoLiMoT.

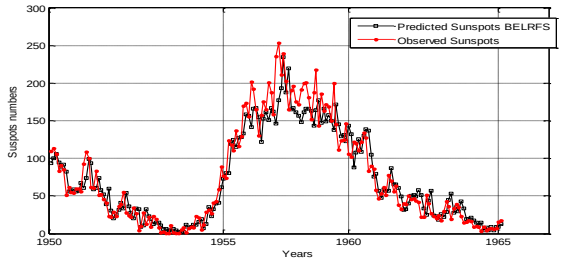

Figure 9. *The Predicted values of monthly sunspots number time series using BELRFS.*

TABLE IV. DIFFERENT METHODS FOR ONE STEP AHEAD PREDICTION OF MONTLY SUNSPOTS FOR SOLARCYCLE 19.

Method	**Specifications**		
	NMSE	***Structure and Epochs***	***Predicted Values***
BELRFS	0.1029	20rules (160)	238 (two months later)
LoLiMoT	0.0885	50rule(50)	228.8464 (One month later)
ELFIS[Lucas et al., 2003]	0.1386	3rules(--)	Between 230 and 240 (one or two months in advance)

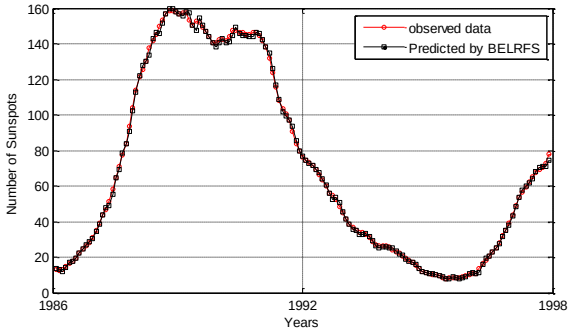

Figure 10. *The Predicted values of smoothed monthly sunspots from 1976 to 1996 using BELRFS and LoLiMoT.*

In the next experiments, the sunspots from January 1999 to January 2001 are tested for recursive prediction. First, the monthly sunspots time series from January 1986 to December 1998 is predicted by BELRFS. Then the obtained results (see Figure 10.) without any correction are used to predict the sunspots of January 1999 to January 2011. The test data includes the peak of solar cycle 23; it has 120.8 sunspots and it occurred in April 2001. The predicted values by the BELRFS are depicted in Figure 11. It is noticeable that BELRFS has the capability to accurately predict the occurrence of solar cycle 23. Table V compares the NMSE of BELRFS when applied for recursive prediction with the obtained results from the studies in [Gholipour et al., 2006b]. It shows that BELRFS can be used as a reliable prediction model.

TABLE V. COMPARISON BETWEEN DIFFERENT DATA DRIVEN METHODS FOR RECURSIVE PREDICTION OF SOLAR CYCLE 23.

Method	**Specifications**		
	NMSE	***Month***	***Predicted peak value***
BELRFS(Recursive predction)	0.0313	April	122.8
LoLiMoT [Gholipour et al., 2006b]	0.046	March	120.9
RBF-OLS[Gholipour et al., 2006b]	0.032	June	120.3

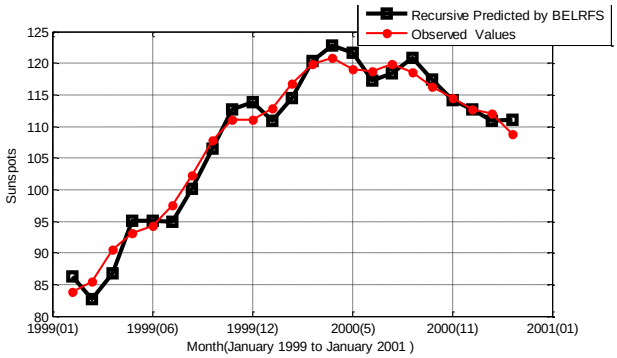

Figure 11 *Recursive prediction of sunspots using BELRFS.*

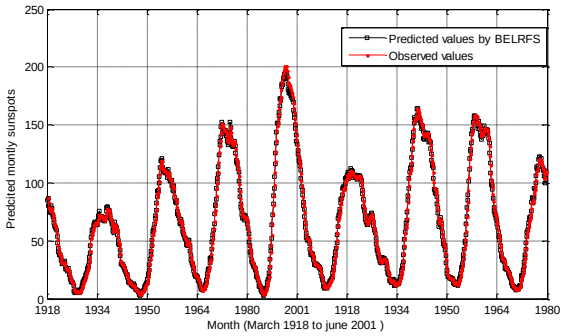

Figure 12. *The predicted value of smoothed monthly sunspots from March 1918 to June 2001 using BELRFS.*

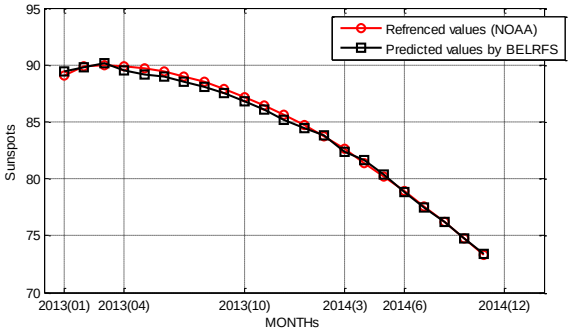

Figure 13. *Using BELRFS for recursive prediction of smoothed monthly sunspots for the test data from January 2013 to January 2014*

As further investigating the performance of BELRFS, the model is applied for the smoothed sunspot number from November 18344 to June 2001. The first 1000 samples are chosen as training data and the next samples are considered

as test data. In this case, BELRFS is tested on the set to obtain comparable results with the studies in [Chandra et al., 2012; Inoussa et al., 2012]. The obtained NMSE from using BELRFS to predict this sunspot time series (November 1834 to June 2001) is equal to 6.64e-4; it is slightly less than the other methods that are mentioned in [Chandra et al., 2012; Inoussa et al., 2012]. However, the Hybrid NARX-Elman RNN [Chandra et al., 2012] and the model that is referred to as Functional Weights Wavelet Neural Network-based state-dependent AuoRegressive (FWWNN-AR) [Inoussa et al., 2012] have predicted this time series more accurately than BELRFS. The reported NMSEs of these methods are 5.23e-4 and 5.90e-4 respectively; which are less than the NMSE of BELRFS. The predicted values by BELRFS are depicted in Figure 13. It can also be seen that the peak points are very accurately predicted by BELRFS.

As the last experiment, we apply BELRFS to predict the sunspot numbers of solar cycle 24, the current solar cycle. Solar cycle 24 stared at 2008 and will end at 2019. First, the sunspots from January 2008 to December 2012 are predicted and then the obtained results without any correction are added to the training samples. Finally, the BELRFS is tested to predict the sunspot from January 2013 to December 2014. The predicted values by BELRFS versus the predicted values in [NOAA, 2012 a] are depicted in Figure 13. Table VI lists the number of sunspots for the peak of solar cycle 24. It has been predicted that the peak of this solar cycle occurs in May 2013 and it has 90 sunspots [NOAA, 2012 b]. Table VI shows that using BELRFS the predicted values are very close to the predicted value in [NOAA, 2012 a].

To evaluate the performance of BELRFS and LoLiMoT, the sunspot numbers for the next four months of 2012 are recursively predicted. Table VII presents the predicted values by BELRFS and LoLiMoT. It indicates that the predicted values of BELRFS are closer to the predicted values in [NOAA, 2012 a]. From all the above experiments, we can conclude that BELRFS is an accurate prediction model for solar activity forecasting.

TABEL VI. COMPARISON BETWEEN DIFFERENT DATA DRIVEN METHODS FOR SOLAR CYCLE 24.

Method	**Specifications**		
	Month	***Predicted peak value***	***NMSE***
BELRFS	May	90.17	0.001
LoLiMoT	May	90.33	3.8e-5
Refrence Model	May	90.33	-----

TABLE VI. COMAPRISON BETWEEN PREDTRED VALUES OF SUNSPOTS FOR NEXT FOUR MONTHS

Method	**Different Methods**		
	BELRFS	***LoLiMoT***	***Predicted values in[NOAA 2012a]***
2012 September	77.2473	76.92	77.3616
2012 October	81.33	79.5434	80.8367
2012 November	85.01	81.7332	84.4843
2012 December	88.05	83.4272	87.7617

4.2 Forecasting geomagnetic storm using Auroral Electrojet Index

As already stated, the AE index is a measure of geomagnetic storms and it can be used to predict space storms. The AE index has been recorded by the World Data Center for Geomagnetism and Space Magnetism (Kyoto University). The BELRFS is evaluated for one minute-ahead prediction of the AE index. For this purpose, the obtained AE index of the first seven days of March 1992 is utilized as training data to predict the AE index of the 9th of March 1992 . Table VIII compares the NMSE, correlation and epochs for one minute-ahead prediction. It can be seen that for short term prediction of the AE index, the prediction error of BELRFS is less than the prediction error of LoLiMoT. The BELRFS predicts the peak values as 1095; while the predicted values by BELRFS is equal to 1105. The observed peak value is 1078. It can be concluded that the BELRFS is more accurate than LoLiMoT in short-term prediction of AE time series. The graph in Figure 14 shows the predicted values of AE index vesus the observed values. It is noticable that the peak values of the AE index are accurately predicted by BELRFS, thus it can be used as a short term alert system for gemagnetic storms.

TABLE VII. COMAPRISON BETWEEN METHODS PREDICT THE AE INDEX.

Method	**Different Methods**		
	NMSE	***Peak value***	***Correlation***
BELRFS	0.0153	1095	0.992
LoLiMoT	0.0241	1105	0.9881

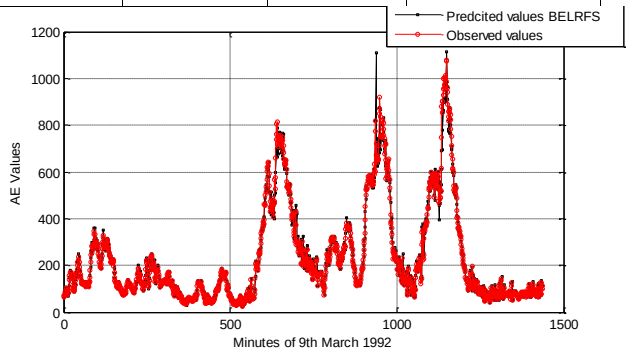

Figure 14. *The predicted AE index using BELRFS.*

5 CONCLUSION AND FUTURE WORK

This paper presents an emotionally-inspired architecture for chaotic time series prediction. The architecture is referred to as BELRFS and consists of one recurrent and two feed forward, adaptive neuro-fuzzy networks. The structure of the BELRFS has been developed using anatomical aspects of emotional learning; while, its function has been illustrated using behavioral aspects of emotional learning. In other words, structurally, the BELRFS mimics the internal interaction of the the limbic system; while, functionally, it imitates the classical conditioning of emotional learning.

The neuro-fuzzy adaptive networks can be constructed using a different number of membership functions. This characteristic increases the flexibility of models and allows one to select the optimal number of membership functions. Some characteristics of the BELRFS are as follows:

1. High prediction accuracy: It has a very good capability to address the uncertainty and unpredictable issues of chaotic time series prediction. It also has the ability to achieve high accuracy prediction using a low number of training data samples.
2. High model complexity: the model complexity of the BELRFS is high, thus it suffers from the curse of dimensionality.
3. High training speed: BELRFS has a fairly fast converge learning algorithm that requires a small number of iterations.

Furthermore, as the obtained results indicate, BELRFS is a fairly accurate prediction model for both long term and short term prediction. Thus, it would be a reliable prediction model for solar activity forecasting, in particular considering the prediction of solar cycle 24.

In the future, the authors would consider adding an optimization method, e.g. genetic algorithm, to find the optimal values of the fiddle parameters of the BELRFS: the initial values of membership functions, the appropriate values for $\boldsymbol{\lambda}$, the vector of loss functions, the number of neighbors, $\boldsymbol{k}$, in nearest neighbor algorithm. In addition, the BELRFS will be presented using other types of fuzzy inference system, e.g. LoLiMoT. We also combine Singular Spectrum Analysis (SSA) with the proposed model to increase the prediction accuracy for long term prediction. We also intend to extend BELRFS with multiple outputs.

The next prediction applications would be other indices of geomagnetic storms, Disturbance storm time (Dst) index and global geomagnetic storm index (Kp index). Moreover, we intend to examine BELRFS as a nonlinear identification method and nonlinear classification model.

ACKNOWLEDGEMENT

First author would like to offer her sincerest thanks to the late Professor Caro Lucas for his inspiration and kind support in supervising me throughout her research process concerning the development the brain emotional learning-based prediction models. First author is also thankful for the financial support of the Knowledge Foundation and CERES (The Centre for Research on Embedded Systems)

In addition, the authors are grateful for accessing sunspot number data and AE index provided by NOAA and World Data Center for Geomagnetism and Space Magnetism, Kyoto University.

REFERENCES

Arbib, M. A. (2002) *The Handbook of Brain Theory and Neural Networks* 2nd ed., MIT Press.

Ardalani-Farsa, M and Zolfaghari, S, (2010) "Chaotic time series prediction with residual analysis method using hybrid Elman–NARX neural networks'', *Neurocomputing*, Vol.73, Issues 13–15, pp.2540-2553.

Babaie, T., Karimizandi, R., and Lucas, C. (2008) "Learning based brain emotional intelligence as a new aspect for development of an alarm system'', *Soft Computing A Fusion of Foundations, Methodologies and Applications, Journal*, Vol. 9, Issue 9, pp.857-873.

Balasundaram, V. and Kennedy, K. (1989) 'A techniques for summarising data access and its use in parallelism enhancing transformations', *Proceedings of ACM SIGPLAN'89 Conference on Programming Language Design and Implementation*, June.

Balkenius, C. and Moren, J. (2001) 'Emotional Learning: A Computational Model of the Amygdala', *Cybernetics and Systems Journal*, Vol. 32, pp. 611-636.

Best, B., (1992) *The Anatomical Basis of Mind*, availble at: http://www.benbest.com/science/anatmind/anatmind.html.

Chandra, R. and Zhang, M. (2012) 'Cooperative coevolution of elman recurrent neural networks for chaotic time series prediction', *Neurocomputing Journal*, Vol. 86, pp.116- 123.

Custodio, L., Ventura, R., Pinto-Ferreira, C. (1999) 'Artificial emotions and emotion-based control systems', *Proceedings of 7th IEEE International Conference on Emerging Technologies and Factory Automation*, pp.1415-1420.

Davis, T. N., and Sugiura, M., (1966), 'Auroral electrojet activity index AE and its universal time variations', Geophys. Res. vol.71, pp.785–801.

Fellous, J. M., Armony, J. L. and LeDoux, J. E. (2003) *Emotional Circuits and Computational Neuroscience*. The Handbook of Brain Theory and Neural Networks, pp. 398-401. The MIT Press, Cambridge, MA

Ferry, B., Roozendaal, B., and McGaugh, J. (1999) "Role of norepinephrine in mediating stress hormone regulation of long-term memory storage: a critical involvement of the amygdala'', *Biological Psychiatry Journal*, Vol. 46, no. 9, pp. 1140-1152.

Gazzaniga, M .S., Ivry, R. B., Mangun, G. R., and Megan, S. (2009), *Cognitive Neuroscience: The Biology of the Mind*, 3rd ed., W. W. Norton & Company.

Golipour, A., Araabi, B. A. and Lucas, C. (2006a) 'Predicting Chaotic Time Series Using Neuraland Neurofuzzy Models A Comparative Study', *Neural Processing Letters*,Vol. 24, no. 3, pp. 217-239.

Gholipour, A., Lucas, C., Araabi, B.N., Mirmomeni, M., and Shafiee, M., (2006b), 'Extracting the main patterns of natural time series for long-term neurofuzzy prediction', *Neural Computing & Applications Journal* .Vol. 16.pp. 383-393.

Golipour, A., Lucas, C., Shamirzadi, D. (2004) 'Purposeful prediction Of Space Weather Phenomena by Simulated Emotional Learning', *modeling Journal*, Vol. 24, pp. 65-72.

Hattan, G., and Porr, B (2012) 'A Computational Model of the Role of Serotonin in Reversal Learning', *Lecture Notes in Computer Science Journal*, Vol.7426, pp.279-288.

Haykin, S. (1999) *Neural Networks: A Comprehensives Foundation*, 2nd ed. Prentice Hall.

Hooker, C. I., Germine, L. T., Knight, R. T., and Esposito, M. D. (2006) 'Amygdala Response to Facial Expressions Reflects Emotional Learning', *Neuroscience Journal*, Vol. 26, no.35, pp. 8915-8930.

Inoussa, G., Peng, H. and Wu, J. (2012) 'Nonlinear time series modeling and prediction using functional weights wavelet neural network-based state-dependent AR model' *Neurocomputing Journal*, Vol. 86, pp. 59-74.

Izeman. A. J., Wolf, J. R. (1998) 'Zurich sunspot relative numbers', *The Mathematical Intelligence Journal*, Vol.7, pp.27-33.

Jang, R., Sun, C. and Mizutani, E. (1997) *Neuro-Fuzzy and Soft Computing: A computational approach to Learning and Machine Intelligence*, Prentice Hall.

Jenkins, J. M., Oatley, K., and Stein, N. L., (1998) *Human emotions : A READER*, Blockwell.

Kandel, E. R., Schwartz, J. H., and Jessell, T. M., (2003), *Principles Of Neural Science, 4th ed.*, McGraw-Hill Medical.

Kappenman, J (2012) 'A perfect storm of Planetary Proportions – How a solarstorm could take down power grids everywhere', *IEEE Spectrum*, February.

Kuremoto, T., Ohta, T., Kobayashi, K., Obayashi, M., (2009a), 'A dynamic associative memory system by adopting amygdala model', *Artificial Life and Robotics Journal*, Vol.13, pp.478–482.

Kuremoto, T., Ohta, T., Kobayashi, K., Obayashi, M., (2009b), 'A functional model of limbic system of brain', in Proceeding of the 2009 international conference on Brain informatics, pp.135-146.

Lucas, C., Shahmirzadi, D., and Sheikholeslami, N. (2004) 'Introducing BELBIC: Brain Emotional Learning Based Intelligent Controller', *International Journal of IntelligentAutomation and Soft Computing (Autosoft)*, Vol. 10, pp. 11-22.

Lucas, C., Abbaspour, A., Gholipour, A., Araabi, B., Fatourechi, M. (2003) 'Enhancing the performance of neurofuzzy predictors by emotional learning algorithm', presented at Informatica (Slovenia), Vol. 27, no. 2 pp.165–174.

Lundstedt, H., (2001) 'Forecasting Space Weather and Effects Using Knowledge-Based Neurocomputing', *Proceedings of ESA Workshop on SpaceWeather*,pp.179–184.

Ma, Q., Zheng, O, Peng, H, Zhong, T., and Xu, L.,' Chaotic Time Series Prediction Based on Evolving Recurrent Neural Networks',*Machine Learning and Cybernetics, 2007 International Conference on* , Vol.6, pp.3496,3500.

Martinez-Rego, D., Fontenla-Romero, O., and Alonso-Betanzos, A., 'A method for time series prediction using a combination of linear models', *Proceedings of the European Symposium on Artificial Neural Network– Advances in Computational Intelligence and Learning*.

Mehrabian, A. R.; Lucas, C., and Roshanian, J. (2006) 'Aerospace Launch Vehicle Control: An Intelligent Adaptive Approach', *Aerospace Science and Technology Journal*, Vol.10, pp. 149–155.

Milasi, R. M., Lucas, C., Araabi, B. N. (2005) 'Intelligent Modeling and Control of Washing Machines Using LLNF Modeling and Modified BELBIC' *Proceeding of* Control and Automation *IEEE International Joint Conference*,pp.812-817.

Miranian, A. and Abdollahzade, M. (2013), 'Developing a Local Least-Squares Support Vector Machines-Based Neuro-Fuzzy Model for Nonlinear and Chaotic Time Series Prediction', *Neural Networks and Learning Systems, IEEE Transactions on* ,Vol.24, no.2, pp. 207-218.Mirikitani, D.T. and Nikolaev, N.,(2010)"Recursive Bayesian Recurrent Neural Networks for Time-Series Modeling," *Neural Networks, IEEE Transactions on* , Vol.21, no.2, pp.262,274,

Moren, J. and Balkenius, C. (2000) 'A computational model of emotional learning in the amygdala', J.A. Mayer, A. Berthoz, D. Floreano, H L. Roitblat, and S.W. Wilson (eds), *From animals to animats*, no. 6 MIT Press, pp. 383–391.

Moren, J. (2001) *Emotion and Learning: A computational model of the amygdala*, Ph.D. disseration, Cognitive Studies, Lund University.

NOAA (2012 a), Predicted Sunspot Number and Radio-Flex. Accessed as. http://www.swpc.noaa.gov/ftpdir/weekly/Predict.txt

NOAA(2012 b), Solar Cycle Progression. Accessed as. http://www.swpc.noaa.gov/SolarCycle/.

Parsapoor,M., Lucas, C. and Setayeshi, S. (2008) 'Reinforcement Recurrent Fuzzy Rule Based System Based on Brain Emotional Learning Structure to Predict the Complexity Dynamic System', *Proceedings Digital Information Management Third IEEE International Joint Conference*, pp. 22-32.

Parsapoor, M., Bilstrup, U. (2012) 'Neuro-fuzzy models, BELRFS and LoLiMoT, for prediction of chaotic time series', *Proceedings of International Symposium on Innovations in Intelligent Systems and Applications (INISTA)*, pp.1-5.

Parsapoor, M., Bilstrup, U. (2012) 'Brain Emotional Learning Based Fuzzy Inference System (BELFIS) for Solar Activity Forecasting', *Proceedings of IEEE International Conference on Tools with Artificial Intelligence (ICTAI 2012, 2012.)*

Rasband. S. N., (1990) *Choatic Dynamics of Nonlinear System*, Wiley-Interscience.

Reisbetg, D., and College, R., (2009) *Cognition Exploring – The Science of the Mind*, 4th ed.,W. W. Norton & Company, U.S.

Rouhani, H., Jalili, M., Araabi, B. N., Eppler, W., and Lucas, C. (2006) 'Brain Emotional Learning Based Intelligent Controller Applied to Neurofuzzy Model of Micro-Heat Exchanger', *Expert Systems with Applications Journal*, Vol.32,pp. 911–918

Schatten, K. H. and W. D. Pesnell (1993), 'An Early Solar Dynamo Prediction: Cycle 23 ~ Cycle 22', *Geophysical research letters, Journal*, Vol. 20, pp. 2275–2278.

Sheikholeslami, N., Shahmirzadi, D., Semsar, E., Lucas, C. (2005) 'Applying Brain Emotional Learning Algorithm for Multivariable Control of HVAC Systems' *Intelligent and Fuzzy Systems Journal*, Vol.16, pp.1–12.

Thompson, R. J. (1993) 'A technique for predicting the amplitude of solar cycle', *Solar Physics Journal*, Vol. 148, pp. 383-388.

Velásquez, J. D. (1998) 'When Robots Weep: Emotional Memories and Decision-Making', Proceesings of the fifteenth national/thent conference on Artifitial Intelligence, pp.70-75.

Zadeh, S. H., Shouraki, S. B., and Halavati, R. (2006) 'Emotional behaviour: A resourcemanagement approach', *Adaptive Behaviour Journal*, Vol.14, pp.357-380.

WEBSITES

http://www.noaanews.noaa.gov/stories2011/20111019_spaceweather.html

http://spaceweathermonitor.com/2011/04/07/an-education-in-solar-activity-and-space-weather/

http://www-star.stanford.edu/~vlf/ejet/electrojet.html

http://www.swpc.noaa.gov

http://en.wikipedia.org/wiki/BELBIC

http://en.wikipedia.org/wiki/Amygdala